Molecular Breeding (2026) 46:119
https://doi.org/10.1007/s11032-026-01742-w

Molecular Breeding

Identification and validation of an important waterlogging QTL on chromosome 6A in spring wheat

Anjali Khadka[1] · **Anja Karine Ruud**[1] · **Tove Kristina Sundgren**[1] · **Tatiana Belova**[1,2] · **Morten Lillemo**[1]

Received: 16 April 2026 / Accepted: 10 November 2026
© The Author(s) 2026

Abstract

Waterlogging is a major abiotic stress affecting wheat production worldwide. In this study, field trials in 2013 and 2014 and subsequent greenhouse experiments in 2023 and 2024 were conducted to identify and validate genomic regions associated with waterlogging tolerance in wheat. Principal Component Analysis (PCA) revealed that foliar chlorosis and overall condition at maturity were major contributors to phenotypic variation under waterlogged conditions. Genome-wide association studies (GWAS) identified *QWl.nmbu-6A*, a major locus on chromosome 6A associated with foliar chlorosis under waterlogging. Haplotype analysis confirmed significant differences in foliar chlorosis between contrasting haplotype groups across both field and greenhouse waterlogging conditions. Further validation using a recombinant inbred line (RIL) population, developed from a cross between GN07560 and Seniorita segregating for the two haplotypes, confirmed the effect of *QWl.nmbu-6A*. Although foliar chlorosis was a reliable indicator under severe waterlogging stress, its predictive power decreased under mild stress, and it did not always reflect the ability of genotypes to recover after waterlogging. Our findings identify *QWl.nmbu-6A* as a promising genomic locus for marker-assisted selection for reduced foliar chlorosis in wheat-growing environments prone to moderate to severe waterlogging. However, its use in breeding should be combined with assessments of post-stress recovery.

Key message

We identified and validated a putatively novel QTL, *QWl.nmbu-6A*, associated with foliar chlorosis under waterlogging stress across field and greenhouse environments, providing an important genomic target for improving waterlogging tolerance in wheat.

Keywords Waterlogging stress · Tolerance · GWAS · Haplotype · QTL · Markers

Extended author information available on the last page of the article

Published online: 19 November 2026

Introduction

Waterlogging stress occurs when soil moisture exceeds field capacity for a longer period (Pampana et al. 2016). This occurs when heavy rainfall is accompanied by poor drainage, causing the air spaces in the soil to become completely saturated with water. Under ideal conditions, soil is composed of approximately 50% solid material and 50% pore space, with the pore space evenly divided between air and water. Under waterlogging conditions, soil pores become fully saturated with water. When the pore volume becomes saturated with water, oxygen diffusion decreases dramatically as gas diffusion is 10^4 times slower in water than in air (Greenway et al. 2006). As microorganisms and plant roots consume the remaining dissolved oxygen through respiration, oxygen levels drop, creating hypoxic or anoxic conditions in the rhizosphere (Nickum et al. 2011). Waterlogging also decreases soil redox potential (Eh). In well-drained, cultivated soil, soil Eh values range from + 300 to + 500 mV (Macías and Camps Arbestain 2010), whereas in waterlogged soil, they decrease to + 100 to -300 mV (Husson 2013). As soil Eh decreases, anaerobic microbes use various electron donor compounds like MnO_2 and Fe $(OH)_3$, reducing them into elemental manganese and iron, respectively. At suboptimal pH levels, these compounds may become abundant in waterlogged soils and reach phytotoxic concentrations (Khabaz-Saberi et al. 2012; Setter et al. 2009; Sundgren 2018).

Wheat is an important cereal crop worldwide (Zohary and Hopf 2000), accounting for 19% of daily caloric intake and 21% of the protein intake globally (Tadesse et al. 2019). The human population is expected to increase by 25% and reach 10 billion over the next 30 years (Hickey et al. 2019). Annual wheat production is expected to reach 1 billion tons by 2050. To meet the projected demand for wheat, it is estimated that the annual genetic gain in wheat yield must increase to an estimated 1.7%. However, efforts to accelerate genetic gain are impeded by global warming and climate change (Tadesse et al. 2019). Waterlogging caused by heavy rainfall and flooding is a major abiotic constraint on wheat production (Zampieri et al. 2017). Approximately 15–20% of global wheat-growing areas are affected by waterlogging annually, resulting in yield losses of 20–50% (Kaur et al. 2020). Flooding events have increased in number, frequency, and intensity in recent decades because of severe and unpredictable rainfall patterns (Masson-Delmotte et al. 2021). As global temperatures continue to rise, these trends are expected to intensify and extend the risk of waterlogging to new areas (Feyen et al. 2012). Major wheat-producing areas in Western Europe and Southern Asia are more likely to be affected by waterlogging than by drought (Zampieri et al. 2017).

Wheat is highly sensitive to waterlogging stress and can experience waterlogging at any time, from germination and seedling stages to booting and grain-filling stages (Mfarrej et al. 2022). Waterlogging stress at early stages, such as germination, seedling establishment, and tillering, usually causes seed rot, reduced seedling survival, leaf chlorosis, and delayed tillering (Ding et al. 2020). Waterlogging at later stages, including heading, flowering or grain-filling, induces leaf senescence and decreases effective spikelet numbers, grain numbers, and grain weight, and finally reduces grain yield (Arduini et al. 2016; Ploschuk et al. 2021). Because of oxygen deficiency, waterlogging stress impairs wheat seed germination and root respiration,

hinders nutrients and water uptake, and limits normal metabolism and photosynthesis (Herzog et al. 2016). The severity of damage increases with the duration of waterlogging (Olgun et al. 2008).

The impacts of waterlogging can be reduced through agronomic measures such as drainage systems (Zhang et al. 2025). Nevertheless, because such events do not occur annually, and their occurrence may deviate from predictions, developing and deploying crop varieties that are resilient across multiple environmental conditions is essential (Khadka 2023). Waterlogging tolerance varies significantly among wheat genotypes (Gardner and Flood 1993; McDonald et al. 2006; Musgrave and Ding 1998), and grain yield losses vary considerably (Setter et al. 1999). The main goal of any breeding program is to improve grain yield, but this trait is complex with low heritability. Consequently, obtaining reliable grain yield data from field trials under waterlogged conditions is challenging. For this reason, researchers often focus on stress-related traits that are highly heritable, easy to measure, and strongly correlated with grain yield to assess waterlogging tolerance in crops (Sundgren et al. 2018). Various stress indicators such as root cortical aerenchyma, rate of germination index, plant height (Yu and Chen 2013), rate of survival (Li et al. 2008), foliar chlorosis and overall condition score (Sundgren et al. 2018), survival rate (Zhou 2011), chlorophyll fluorescence (Pang et al. 2004), the visual score of root-color (Musgrave and Ding 1998), number of tillers at maturity (Collaku and Harrison 2002), and shoot or root biomass (Ballesteros et al. 2015) etc. have been used to study waterlogging tolerance in wheat. Chlorosis percentage is one of the best phenotypic predictors of yield for assessing wheat waterlogging tolerance under field waterlogging conditions. This trait is significantly correlated with grain yield and can be measured easily at early developmental stages (Sundgren et al. 2018).

Identifying tolerant germplasm and associated quantitative trait loci (QTL) is important for improving waterlogging tolerance in wheat. Improving wheat waterlogging tolerance through marker-assisted selection (MAS) depends on the identification of genetic markers that are tightly linked to the target trait. QTL mapping is an effective method for investigating the genetic basis of traits and identifying genomic regions containing significant QTL (Sundgren et al. 2018). Several QTL associated with waterlogging tolerance have been identified in wheat. Ballesteros et al. (2015) mapped 48 QTL at the vegetative stage, with a major QTL on chromosome 1D explaining 24% of the variance in chlorophyll content. Yu et al. (2014) found 32 QTL across 14 chromosomes, including a major one for germination index on 7 A explaining 23.9% of the variance. The QTL reported in these studies were primarily identified in recombinant inbred line (RIL) populations. QTL identified using RIL populations may have low mapping resolution because few numbers of recombination events occur in such populations. Moreover, genetic variation is also limited to that between the parents (Ingvarsson and Street 2011), resulting in low mapping resolution and high intra-chromosomal linkage disequilibrium (LD) (Flint-Garcia et al. 2003). In contrast, genome-wide association studies (GWAS) use natural populations in which numerous recombination events have occurred over many generations (Korte and Farlow 2013). Such populations usually have high allelic diversity and greater mapping resolution (Zhu et al. 2008). However, GWAS have limitations associated with population structure (Breseghello and Sorrells 2006) and multiple -testing problems (Gupta et al. 2014) which need to be carefully considered.

Over the past decade, several GWAS models have been developed to improve genetic studies, including MLM, CMLM, EMMA, ECMLM, SUPER, FarmCPU, and BLINK (Huang et al. 2019; Liu et al. 2016; Yu et al. 2006; Zhang et al. 2010). Each model comes with its own pros and cons. The criteria for choosing among these models include statistical power, computing efficiency, and the ability to avoid false-positive QTL detection. The Mixed Linear Model (MLM) was previously popular because of its ability to correct population structure using a kinship matrix and principal components. However, it was found to be computationally intensive and, in some cases, produced many false negatives (Sandhu et al. 2024). Liu et al. (2016) developed FarmCPU, a multilocus model that iteratively alternates between fixed and random-effects models to reduce false positives. Huang et al. (2019) introduced BLINK, another multi-locus model that uses LD information to improve statistical power relative to FarmCPU and reduces computation time by replacing the random-effects model (REM) with a fixed-effects model (FEM) and applying the Bayesian information criteria (BIC). These models are advanced in GWAS analysis compared to conventional GLM and MLM models and are often implemented in widely used software such as PLINK, TASSEL, GAPIT and rrBLUP (Bradbury et al. 2007; Endelman 2011; Lipka et al. 2012; Purcell et al. 2007). Cloning or fine mapping of identified QTL in wheat remains challenging, primarily due to the large size of the wheat genome and the complex genetic basis of waterlogging tolerance (Tanin et al. 2022). Therefore, validating and fine mapping of identified QTL are particularly important for their application in marker-assisted breeding programs for improving waterlogging stress tolerance (Sundgren 2018).

Field-based screening for waterlogging tolerance remains essential for capturing plant responses under natural conditions. However, maintaining uniform water-table levels across plots is challenging, resulting in variable stress intensity (Sundgren 2018). In addition, fluctuations in temperature, pH, nutrient availability, and other biotic and abiotic factors reduce experimental uniformity and reproducibility. Field experiments are also labor-intensive, time-consuming, and costly. To complement field evaluations, controlled-environment screening methods such as greenhouse or growth chamber screening are increasingly used. Among these, starch-based greenhouse waterlogging methods provide an effective way to simulate hypoxic soil conditions. The addition of starch stimulates microbial respiration, leading to oxygen depletion in the root zone and mimicking the anaerobic conditions observed under field waterlogging. This screening method allows for a more controlled and reproducible assessment of genotypic responses to waterlogging. Studies have shown that a 0.1% (m/v) starch solution can mimic waterlogging conditions in barley by creating a strongly reducing environment (Byrne et al. 2022; Mano and Takeda 2012). Thus, combining field-based screening with controlled-environment validation provides a strong framework for identifying and confirming genetic loci associated with waterlogging tolerance.

Here, we report a GWAS that identified an important QTL region on chromosome 6A (610–613 Mb), designated *QWl.nmbu-6A*, associated with foliar chlorosis under field waterlogging conditions in 2013 and 2014. Foliar chlorosis was considered a proxy indicator of the plant stress response to waterlogging. To examine the reproducibility of the QTL effect under controlled conditions, we conducted two

greenhouse experiments using a starch-based waterlogging method. The first experiment, conducted in 2023, included a selected subset of wheat genotypes carrying contrasting *QWl.nmbu-6A* haplotypes previously identified in the field experiments. We also developed RILs from a cross between GN07560 and Seniorita, the parental lines carrying contrasting *QWl.nmbu-6A* haplotypes. The second experiment, conducted in 2024, included selected RILs carrying contrasting haplotypes at this locus. Together, these experiments were designed to evaluate the consistency of the association between *QWl.nmbu-6A* and foliar chlorosis across years and between field and controlled greenhouse environments.

Materials and methods

Field experiments

Plant material

Genotypes used for field waterlogging experiments in the years 2013 and 2014 have been described in detail by Sundgren et al. (2018). In brief, the wheat genotypes under study were subsets of the NMBU spring wheat panel (MASBASIS) that consist of advanced breeding lines, cultivars, landraces, and various crossing parents. A total of 181 lines of wheat were tested across the experimental years 2013 and 2014. Of which, 107 genotypes were tested for both years. Population structure of the genotypes under study followed their geographic origin, dividing the collection into two sub-populations. One sub-population comprised adapted lines while the other sub-population included exotic lines (see Supplementary material, Fig. S1).

Field phenotyping

Field experiments for waterlogging tolerance were conducted in the years 2013 and 2014 at Vollebekk experimental station of the Norwegian University of Life Science (NMBU), Ås, Norway. Details of these field experiments and their results have been explained by Sundgren et al. (2018). Briefly, field experiments were conducted using hill plots with 4 g of seeds in each plot. Experiments were designed as alpha lattice with three replications under both waterlogged and control conditions. To create artificial waterlogging conditions, levees and trenches were prepared using an excavator surrounding the waterlogging experiments. The levees were strengthened with durable plastic. Once the genotypes reached the third leaf stage, water was introduced into the experiment by using irrigation pipes. To make constant water level above the soil surface, a gentle water flow was maintained throughout the treatment. Ten and thirteen days of waterlogging were maintained in the year 2013 and 2014, respectively (Sundgren et al. 2018).

Phenotypic traits measured in both experimental years included percentage of foliar chlorosis, relative plant height, heading delay, and overall condition. In addition to these traits, green biomass after drainage and relative head numbers were also measured in 2014. Details of their measurements were explained by Sundgren et al.

(2018). The percentage of foliar chlorosis was measured once clear distinction among wheat genotypes was observed. Chlorosis was assessed on a plot basis using visual estimation and scored on a 0-100% scale, where 0 represented no visible chlorosis and 100 represented complete chlorosis of the canopy. The percentage was estimated based on the proportion of chlorotic leaf area relative to the total leaf area within each plot. In cases where necrosis was observed, affected leaves were considered to indicate advanced damage and were assigned proportionally higher chlorosis scores during visual assessment. Similarly, the overall condition score (OC) was recorded at maturation on the scale of 1–10, where a score of 1 was considered lowest OC. The overall condition score was assessed by considering spike size, biomass, and overall vigor (Sundgren et al. 2018).

Greenhouse experiments

Greenhouse experiments were conducted in a semi-controlled greenhouse, at the Centre for Plant Research in Controlled Climate (SKP) at the Norwegian University of Life Sciences, Ås, Norway. Plants were grown at an average day/night temperature of 18/15°C with relative humidity (R.H.) of 60% inside the semi-controlled greenhouse. Supplemental HPS lighting maintained a 16-h photoperiod.Two different sets of genotypes were tested in two different experiments to evaluate the haplotype effect of the major QTL *QWl.nmbu-6A* for chlorosis. In the first experiment, a subset of twenty genotypes from MASBASIS with contrasting haplotypes were selected based on GWAS results from the field trial. Out of twenty selected genotypes, eleven of them belonged to haplotype CGT, and the remaining nine were from haplotype TAG (see Supplementary material, Table S3). Haplotype CGT was associated with a lower level of chlorosis while haplotype TAG was associated with a higher level of chlorosis. Seeds harvested from a MASBASIS field trial in 2019 were used as seed sources for this experiment.

Two lines, GN07560 and Seniorita with contrasting haplotypes for *QWl.nmbu-6 A* were crossed and F_6-derived RILs were developed by single seed descent (SSD). From this population, eighteen RILs were selected for the second greenhouse experiment plus two parental lines. Of the selected RIL lines, half belonged to haplotype CGT, and the remaining half belonged to haplotype TAG (see Supplementary material, Table S4).

Experimental design methodology and phenotyping

The greenhouse experiments were conducted using RL98-Ray Leach cone-tainer trays (Stuewe & Sons Inc, 31933 Rolland Dr, Tangent, OR, United States, Oregon), with dimension $60.96 \times 30.48 \times 17.15$ cm used as experimental units. The individual cones were filled with layers of stones, peatmoss, and sand to prevent them from floating inside the plastic boxes during the starch waterlogging treatment (Fig. 1A). Twenty wheat genotypes were distributed in a Complete Randomized Block Design in these trays for both control and starch-waterlogging treatments with three replications each. In our experiments, starch (0.1% m/v) solution was prepared and kept in simple Smart StoreTM Classic 70 (Orthex Group, Espoo, Suomalaistentie 7, Finland)

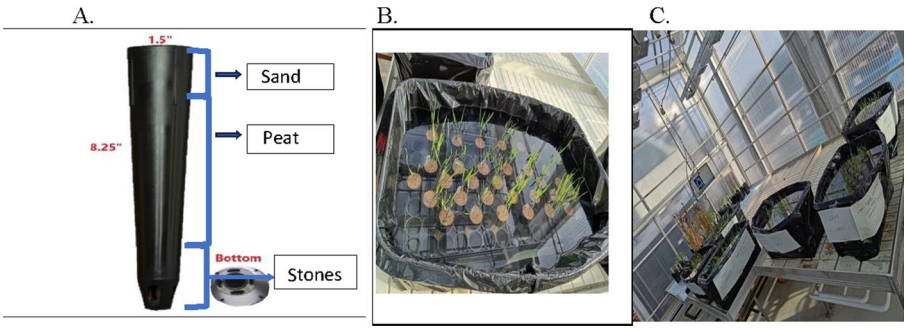

Fig. 1 (**A**) SC10R – Ray Leach Super Cell Classics showing layers of stones, peat and sand used for cone stabilization. The figure was modified from the original taken from (https://stuewe.com/product/ray-leach-super-cell-recycled/). (**B**) Overhead view of cone-tainer tray inside white box wrapped with polythene. (**C**) Overall view of the waterlogging experiment with starch waterlogging and control where each black box represents one replication

white plastic boxes (outer measurements 72 *40 * 38 cm, inner measurements 59.1 *30 * 33.2 cm, volume 70 L). The plastic boxes were wrapped with black polythene cover before pouring starch solution into them. The waterlogging treatment started when plants reached the third leaf stage. The trays were then put into plastic boxes with a starch solution as shown in Fig. 1B. The water level above the soil surface was maintained at 8.5 cm throughout the waterlogging treatment, which was discontinued after 18 days of waterlogging. In case of control treatment, normal water was used instead of starch solution.

Foliar chlorosis was measured after there was visible distinction among genotypes under study. Genotypes with necrosis along with chlorosis were given a higher percentage score of chlorosis. Details of this greenhouse experiment were previously explained by Khadka (2023).

Soil type and soil redox potential

Field experiments were conducted on a mollic gleysol characterized by poor drainage, whereas in greenhouse experiments Sphagnum-based white moss peat (Vekst-torv, Norgro, Norway) with a pH of 5.0–6.0 as the growth medium was used. Soil redox potential (Eh) was measured under waterlogged conditions in both field and greenhouse experiments using a platinum electrode (HI 3032) connected to a portable millivolt/pH meter (HI 8424) (Hanna Instruments, Inc., Woonsocket, RI, USA). The electrode was calibrated using a standard redox buffer solution (220 ± 5 mV at 25 °C) prior to measurements. Measurements were taken at a depth of 4–5 cm, and average values from multiple points within each replication were calculated. In the field experiment, soil physical and chemical properties were determined using standard procedures to ensure that nutrient contents (P, K, Ca, Mg, Mn), pH, total carbon, and nitrogen were similar between waterlogged and control experiments. Soil infiltration rate was also assessed using standard protocols. Details of soil characteristics and measurement procedures were previously described in detail by Sundgren et al. (2018).

Genotyping

The wheat lines were genotyped using DNA extracted from leaf tissue and the TraitGenetics Illumina 25 K SNP array (TraitGenetics GmbH, Seeland OT Gatersleben, Germany,). There were 22,205 SNPs counts before filtering the data. Monomorphic and failed markers were filtered out while heterozygous genotypes were considered as missing data. Markers with more than 10% missing data and those with a minor allele frequency ≤ 0.05 were removed. Final genotype datasets after filtering and removing duplicate markers consisted of 18,578 markers in the 25 K SNP dataset before association analyses (Lin et al. 2023). Physical marker positions were interpreted using the IWGSC Chinese Spring RefSeq v2.1 assembly.

Statistical analysis

Software Rstudio (version 4.4.2) was used for analysis of all the data obtained. Phenotypic data of all measured traits were analyzed through linear mixed model $Y_{ij} = \beta 0 + v_i + u_{0j} + \varepsilon_{ij}$. Here, Y_{ij} is the observed value of the "trait" for the i-th genotype and j-th replication. β0 is the fixed intercept, which captures the overall mean of measured trait across all genotypes and replications, v_i represents the random intercept for the i-th genotype, which denotes the deviation from the overall mean value of measured trait specific to that genotype, u_{0j} represents the random intercept for the j-th replication, that covers the deviation from the overall mean of measured trait specific to that replication, ε_{ij} denotes the residual error term, which accounts for the random variation in the observed in measured trait. This linear mixed model was fitted using the lmer () function in the "lme4" (version 1.1.37) package in R studio. This model considers genotypes and replication as random effects in relation to the dependent variable, measured phenotypic trait. Estimated random effects also known as Best Linear Unbiased Predictions (BLUPs) for each level of the genotypes factor, were calculated using the ranef () function inside the "Lme4" package. BLUP values of each measured phenotypic trait were used for further analysis. Pearson´s correlation coefficient was measured among the measured traits of both years using R package "metan" (version 1.19.0). Welch's two-sample t test was done to compare the estimated genotype means of chlorosis percentage (BLUPs) between the two haplotype groups.

Association analysis

GWAS was conducted by GAPIT3 (Liu et al. 2016; Wang and Zhang 2021) using three different models MLM (Yu et al. 2006), FarmCPU (Liu et al. 2016) and BLINK (Huang et al. 2019) in R environment (version 4.4.1). GAPIT3 was directly sourced from "http://zzlab.net/GAPIT/gapit_functions.txt". Bonferroni threshold was ca lculated using the function "CalcThreshold" implemented in R package "RAINBOWR" (Hamazaki and Iwata 2020), with a significance level of 0.05 and method = "Bonf". Based on 18,578 markers, the genome-wide significance threshold was $-\log_{10}(P) = 5.57$. Manhattan plots obtained from GAPIT results were customized

using R package "ggplot2". TASSEL version 5.2.9 (Bradbury et al. 2007) was used to calculate pairwise Linkage disequilibrium (LD) between markers on each chromosome by using full-matrix option. For haplotype construction, hapmap file and results obtained from LD analysis from TASSEL5 was analyzed in R version 4.4.2 to construct haplotype based on significant markers in high LD (R^2 >0.85). The list of markers used for haplotype construction and their R^2 values, physical chromosome positions, and their p-values is given in Table 1. Using multi-locus models like BLINK and FarmCPU only one marker will be picked per chromosome region per phenotype.

BLINK was selected as the primary model for interpretation because it is a multilocus GWAS method that uses linkage disequilibrium (LD) and the Bayesian information criterion to select pseudo-QTNs as covariates (Huang et al. 2019). By using LD rather than predefined genomic bins, BLINK avoids assumptions about the genomic distribution of causal variants. This feature was relevant because the markers defining *QWl.nmbu-6A* occur within a narrow interval and are in strong LD. Evaluations using simulated and empirical datasets have shown that BLINK can improve statistical power and computational efficiency while controlling false-positive associations under the conditions examined (Huang et al. 2019). GAPIT3 similarly describes BLINK as a powerful and computationally efficient method, while emphasizing that model performance depends on population structure and trait architecture (Wang and Zhang 2021). FarmCPU and MLM were retained as complementary models. FarmCPU is an alternative multilocus analysis that iteratively applies fixed- and random-effect models (Liu et al. 2016), whereas MLM provided a more conservative analysis accounting for population structure and kinship (Yu et al. 2006). Model sensitivity was assessed using zero, one and two principal components in GAPIT3. No external kinship matrix was supplied; where required, kinship was estimated internally from the filtered genotype matrix using the default VanRaden method.

Genome-wide significance was determined using a Bonferroni-corrected threshold of $-\log_{10}(P)=5.57$, based on 18,578 tested markers. Bonferroni correction was selected instead of FDR to provide conservative control of the family-wise error rate because the analysis focused on identifying a limited number of high-confidence loci for subsequent validation. This approach may reduce the power to detect loci with smaller effects because of correlations among markers arising from LD. A threshold of $-\log_{10}(P)=3$ was therefore used only to identify suggestive associations and assess their consistency across models and sensitivity analyses. Associations exceeding only this exploratory threshold were not considered confirmed QTL without additional supporting evidence.

Table 1 The marker ID of 25 K SNP markers that were used to construct haplotypes along with their pairwise Linkage Disequilibrium (LD) values, and their physical positions on chromosome 6A (Pos)

Marker ID	Position (bp)	Pairwise LD (R^2)	
GENE-4021_496	610,349,860	*GENE-4021_496 - AX-95182345*	0.94
AX-95182345	611,661,202	*GENE-4021_496 - AX-94634087*	0.85
AX-94634087	612,329,159	*AX-95182345 - AX-94634087*	0.88

Haplotype analysis

Phenotype data from 2013 to 2014 and genotype data from the 25 K SNP chip were used for GWAS using FarmCPU, BLINK and MLM models. Consistently significant markers were selected from the GWAS results. Only those SNPs above Bonferroni threshold ($-\log_{10}(P)=5.57$) were considered significant. Markers that were in high LD with a major significant marker were used for haplotype construction. Genotyping of RILs derived from GN07560 ×x Seniorita was also done by the TraitGenetics 25 K wheat SNP chip. The genotype data was used to select RILs with contrasting *QWl.nmbu-6A* haplotypes for validation in greenhouse waterlogging conditions. The full genotyped population comprised 257 RILs and the two parental lines. Based on *GENE-4021_496*, *AX-95182345*, and *AX-94634087*, 119 RILs carried the CGT haplotype, 124 carried the TAG haplotype, 10 showed recombinant or mixed haplotypes within the marker-defined interval, and 4 had missing or ambiguous marker calls.

Results

Correlation

Pearson's correlation analysis showed that chlorosis and heading delay were significantly positively correlated with each other in 2013, while both traits were significantly negatively correlated with plant height and overall condition, respectively. In 2014, chlorosis showed weak negative or positive non-significant correlations with heading delay, plant height, overall condition, head number, green biomass at 15 days post drainage (Greenbiomass15_14), and green biomass at 5 days post drainage (Greenbiomass5_14). However, heading delay had significant negative correlations with overall condition, head number, Greenbiomass5_14, and Greenbiomass15_14, while its correlation with plant height was negative but non-significant (Fig. 2).

Both Greenbiomass5_14 and Greenbiomass15_14 were significantly positively correlated with each other, overall condition, and head number. Between years, chlorosis, heading delay, and plant height showed significant positive correlations, while overall condition showed a weak, non-significant correlation.

Principal component analysis

Principal component Analysis (PCA) of the phenotypic data showed that PC1 explained 48.2% and 50.9% of variance in 2013 and 2014, respectively. Similarly, PC2 and PC3 explained 24.5% and 15.6% in 2013 whereas 15.3% and 13.1% of the variance in 2014 respectively (Fig. 3). In 2013, the major contributors to PC1 were overall condition (29.8), heading delay (27.5), and chlorosis (24.6). Overall condition had negative loading while chlorosis and heading delay had positive loading on PC1. Relative contribution of plant height was highest on PC2 (46.4) followed by chlorosis (25.7) and heading delay (17.9) while overall condition had least relative contribution to PC2 (9.8). Similarly, chlorosis had highest relative contribution to

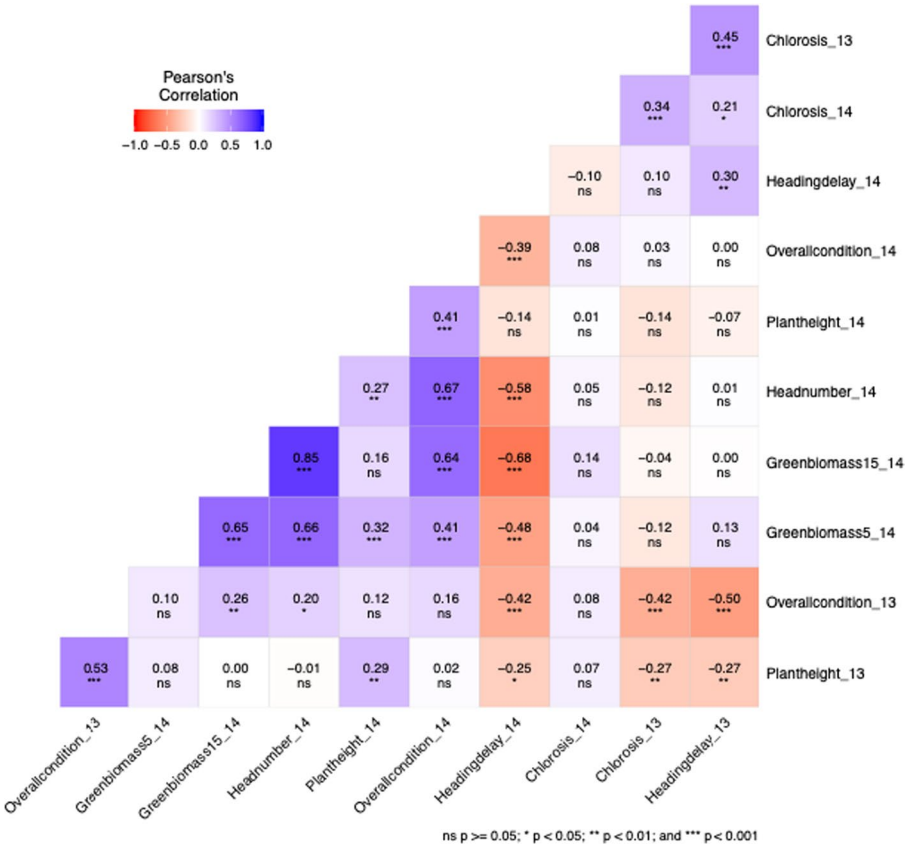

Fig. 2 Correlation matrix between the phenotypic traits that were recorded in experimental year 2013 and 2014

PC3 (41.8) followed by heading delay (32.5), whereas plant height and overall condition had small relative contribution to PC3. In 2014, PC1 was mainly influenced by GBM15 (20.3), relative head number (19.8), overall condition (17.6), GBM5 (16.7), and heading delay (16.4), while chlorosis had a minimal contribution (1.1). GBM5, GBM15, head number, and overall condition had negative loadings on PC1, whereas heading delay showed a positive loading. Similarly, chlorosis had the highest relative contribution to PC2 (40.5) in 2014, followed by plant height (33.08). All the remaining traits showed moderate to small contribution to PC2. For PC3, chlorosis remained the dominant trait (31.4), followed by plant height (33.4) and heading delay (10.8), whereas traits such as green biomass and overall condition had very low contributions to PC3 (see supplementary material, Table S5).

Overall condition at maturity contributed most to PC1 in both years but showed weak contributions to PC2 and PC3. Chlorosis contributed to all three principal components in 2013, with the highest influence on PC3 followed by PC2 and PC1. In contrast, in 2014, chlorosis was the dominant contributor to PC2 and one of the main

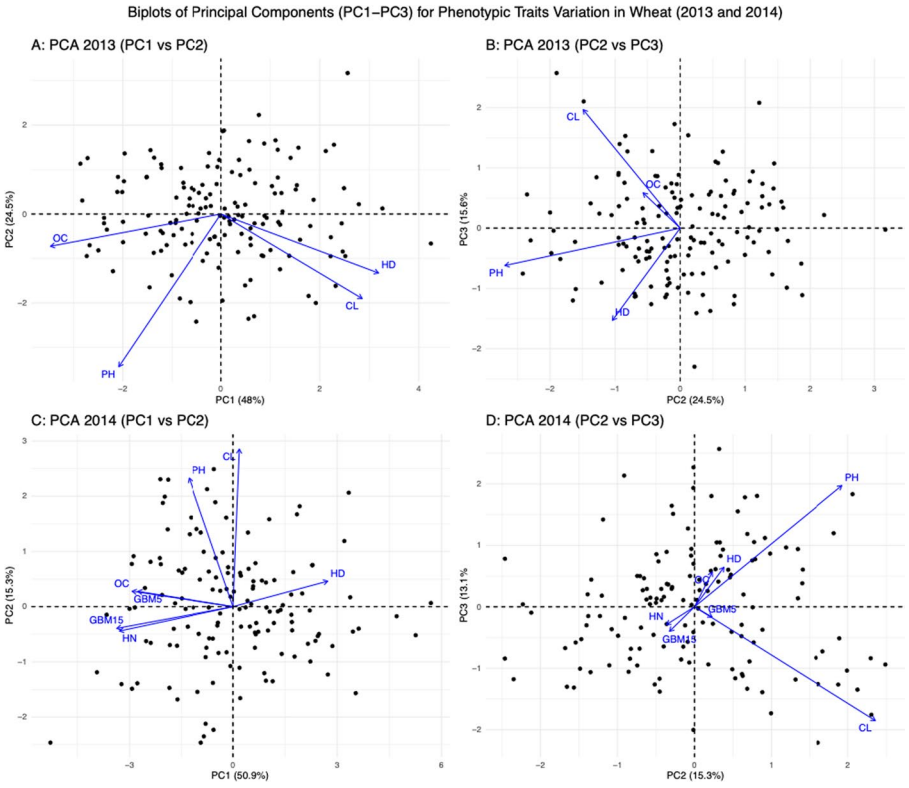

Fig. 3 Biplot of Principal Component Analysis (PC1-PC3) of 138 wheat genotypes and phenotypic traits recorded for field experiment in year 2013 (**A** and **B**) and year 2014 (**C** and **D**). Scores in the biplot represented by black circles are wheat genotypes under study. Arrows in the biplots indicate phenotypic traits that were measured in that year. OC: Overall condition, PH: Relative plant height, CL: Chlorosis percentage, HD: Heading Delay, HN: Head Number, GBM5: Green-biomass five days after drainage, GBM15: Green-biomass fifteen days after drainage. PC1 and PC2 were previously published by Sundgren et al. (2018)

contributors to PC3, but its influence on PC1 dropped sharply. In contrast to 2013, traits like green biomass, heading delay and overall condition were found to be main contributors to PC1 in 2014.

Analysis of variance (ANOVA) and heritability of chlorosis

Results of ANOVA showed that there was highly significant genotype effects for chlorosis in both years 2013 ($F = 2.37$, $p = 2.11 \times 10^{-7}$) and 2014 ($F = 7.93$, $p = 3.33 \times 10^{-36}$), indicating significant variation among the tested wheat genotypes in each year. Replication effects were also significant, with $F = 5.83$ ($p = 3.53 \times 10^{-3}$) in 2013 and $F = 3.35$ ($p = 3.69 \times 10^{-2}$) in 2014. Block effects showed significance in both years as well, with $F = 1.53$ ($p = 4.21 \times 10^{-2}$) in 2013 and $F = 2.29$ ($p = 2.50 \times 10^{-4}$) in 2014. Broad-sense heritability (H^2) for chlorosis was 0.59 in 2013 and 0.87 in 2014 and while it was 0.40 when estimated across years (see supplementary material S4, S5 and Table S1).

Broad-sense heritability for chlorosis was 0.59 in 2013 and 0.87 in 2014 but decreased to 0.40 in the combined analysis across years. Genotype × year variance was not included in the individual-year analyses because each analysis contained only one year; consequently, this interaction could not be estimated. In contrast, the combined analysis included both years and allowed genotype × year interaction to contribute to the total phenotypic variance.

Genome wide association studies

PC scores (PC1-PC3) based on PCA of the studied traits were used as phenotypes for GWAS analysis, along with chlorosis. Peaks above or at the Bonferroni threshold level ($-\log_{10}(P)=5.57$) and the exploratory threshold level ($-\log_{10}(P)=3$) were taken into consideration in the results.

For 2013, the results of BLINK GWAS on PC1 showed no significant peaks at the stringent Bonferroni threshold. However, peaks on chromosomes 1D and 2D were observed above the exploratory level, while several peaks on 2B, 4A, 5 A, and 5B were detected at the exploratory threshold (Fig. 4A). For PC2, a significant peak on chromosome 6A (*AX-95092538*, Pos = 613.77 Mbp, $-\log_{10}(P)=5.80$) exceeded the Bonferroni threshold ($-\log_{10}(P)=5.57$). In addition, a peak on chromosome 1B was observed above $-\log_{10}(P)=4$. Several other peaks on chromosomes 3A, 3B, 5 A, 6B, 7A, and in unmapped regions were detected above the exploratory threshold (Fig. 4B). For PC3, there were no significant peaks above the Bonferroni threshold. However, several peaks on chromosomes 1 A, 6B, and 7A were observed above the exploratory level, and peaks at 1D and in unmapped regions were detected at the exploratory threshold (Fig. 4C).

GWAS results for chlorosis in 2013 revealed no significant peak above the Bonferroni threshold. However, a peak was detected on chromosomes 1B above the exploratory threshold, and on chromosome 2B and 6B at the exploratory threshold (Fig. 4D). Similarly, peaks on chromosome 2D, 3B, 6A, 7A, and unmapped regions were detected slightly below exploratory threshold (Fig. 4D).

Similarly, in 2014, GWAS results using the BLINK model for PC1 showed a peak on chromosome 3B above the Bonferroni threshold. Peaks on chromosomes 1B, 2 A, 5B, and in unmapped regions were observed at the exploratory threshold (Fig. 5A). For PC2, significant peaks above the Bonferroni threshold were detected on chromosomes 6A (*AX-158587917*, pos = 612.30 Mbp, $-\log_{10}(P)=6.29$) and 7B. Likewise, peaks on chromosomes 3B, 5B, 7A, and in unmapped regions were observed above the exploratory threshold, while peaks on chromosomes 3A, 4A, 5A, and 6D were detected slightly below it. For PC3, several significant peaks were detected above and at the Bonferroni threshold, including on chromosome 6A (*GENE-4021_496*, pos = 610.35 Mbp, $-\log_{10}(P)=11.91$), 6D ($-\log_{10}(P)=8.04$) and on 5A ($-\log_{10}(P)=5.68$) while peaks in unmapped regions were observed at the Bonferroni threshold. Additionally, several peaks just below the Bonferroni threshold were detected on chromosomes 2A, 2B, 7B along with peaks on chromosomes 1A, 1B, 5B, and 5D just above the exploratory threshold while peaks on chromosome 3B, 5B and unmapped regions were observed slightly below it.

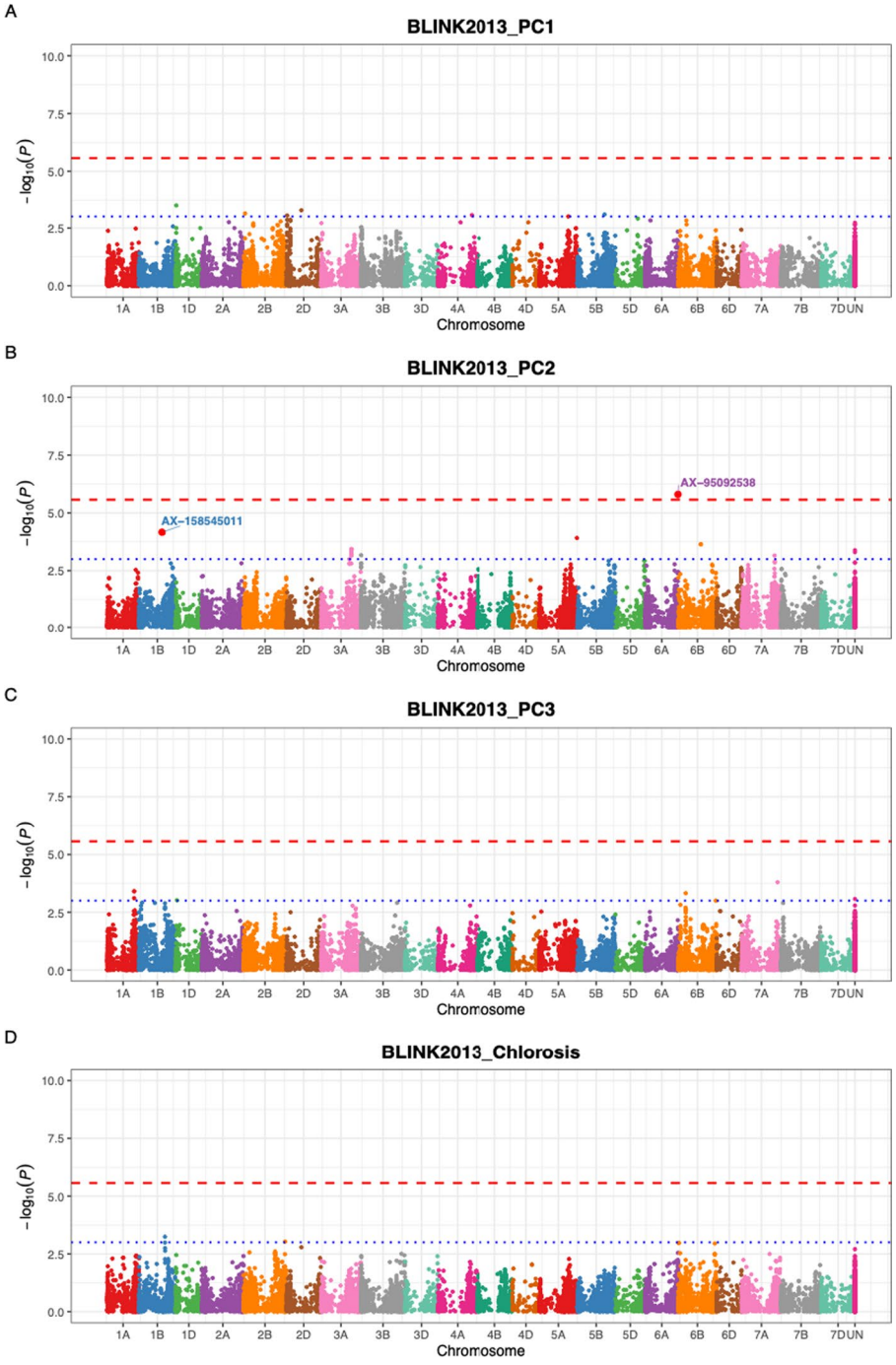

Fig. 4 Manhattan plots for GWAS analysis of Principal components PC1 (**A**), PC2 (**B**), PC3 (**C**) and Chlorosis (**D**) for the studied wheat genotypes under field waterlogging condition in experimental year 2013 using BLINK model

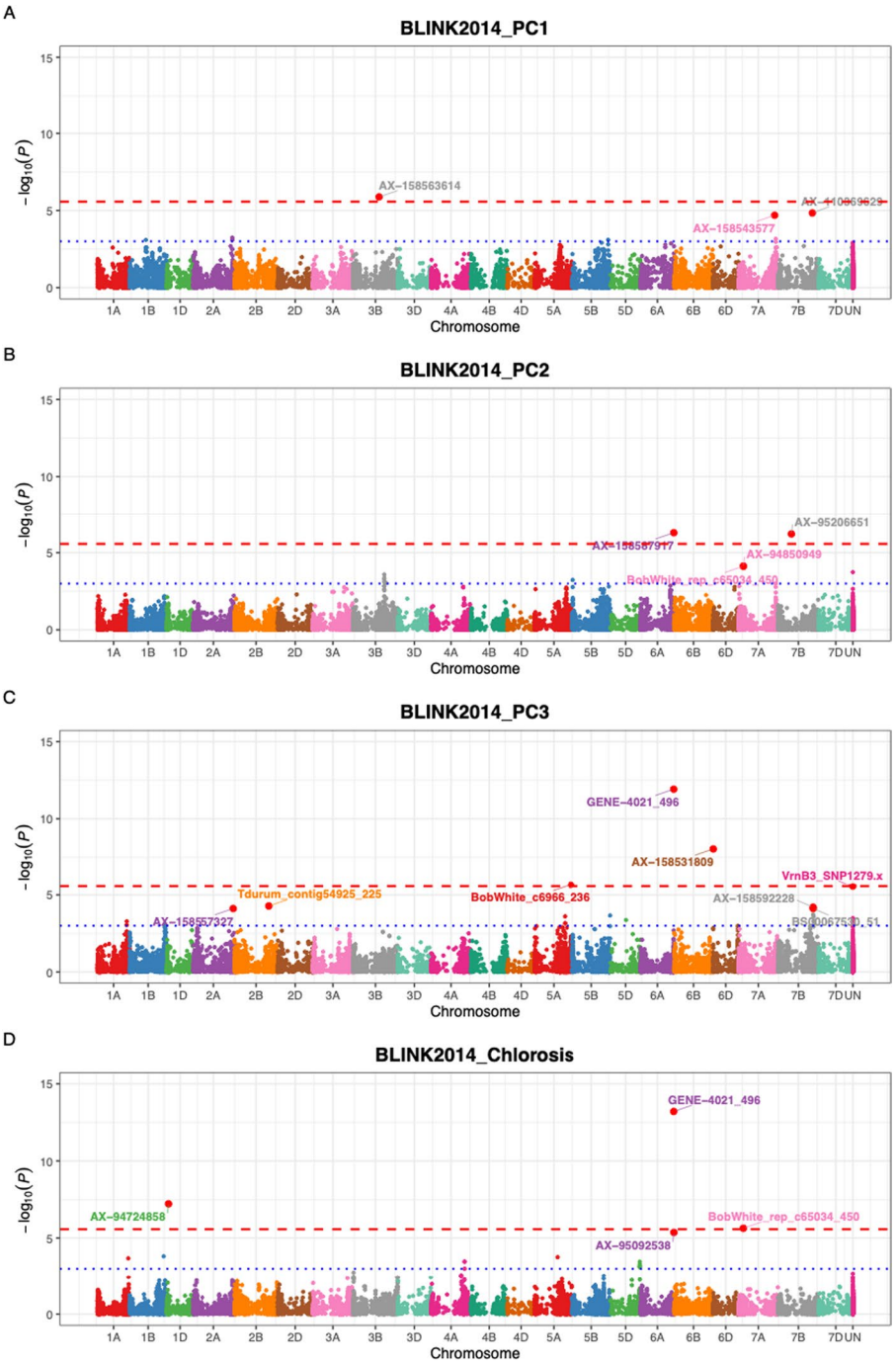

Fig. 5 Manhattan plots for GWAS analysis of Principal components PC1 (**A**), PC2 (**B**), PC3 (**C**) and Chlorosis (**D**) for the studied wheat genotypes under field waterlogging condition in experimental year 2014 using BLINK model

Similarly, GWAS results using the BLINK model for foliar chlorosis in 2014 revealed significant peaks above the Bonferroni threshold on chromosomes 6A (*GENE-4021_496*, pos = 610.35 Mbp, $-\log_{10}(P) = 13.02$) and 1D ($-\log_{10}(P) > 5.57$), along with a peak on chromosome 7A ($-\log_{10}(P) = 5.57$) at the Bonferroni threshold. Additional peaks were observed on chromosomes 1 A, 1B, 4 A, 5A, and 5D above the exploratory threshold.

The consistent QTL on chromosome 6A (610–613 Mbp) was also found for foliar chlorosis using FarmCPU and MLM (see supplementary materials, Fig. S9). This QTL was also confirmed using different PC counts for population structure in different GWAS models (see supplementary materials, Fig. S12 and S13) in 2014. On top of that, it was consistently observed through all GWAS models for chlorosis in 2014 when exotic lines were removed from the population (see supplementary materials, Fig. S14, S15 and S16). Given the importance of this QTL, we designated it as *QWl.nmbu-6A*, following the QTL nomenclature guidelines in wheat (Boden et al. 2023). Even though other QTL on several chromosomes were identified, they were either model specific, or their significance levels were lower across different models. From all the GWAS results on different PCs (mainly PC2 in both 2013 and 2014 and PC3 in 2014) along with GWAS on the chlorosis trait itself, it was distinctly clear that the genomic region on chromosome 6A (610–613 Mbp) was highly relevant for further investigations. Therefore, haplotypes of this locus were constructed using 25 K markers. Notably, one SNP on chromosome 6A (*GENE-4021_496*) was found to be consistently significant across all the models BLINK, FarmCPU and MLM (see supplementary materials, Fig. S9) using foliar chlorosis as phenotypic trait in 2014 with $-\log_{10}(P)value > 12$ which is well above the Bonferroni threshold. Nearby SNPs in high LD with *GENE-4021_496* were used for construction of haplotypes (Table 1). Two of the markers were *AX-95182345* ($R^2 = 0.94$) and *AX-94634087* ($R^2 = 0.85$). Detailed information about these markers can be found in Table 1 with physical position of those SNP markers on chromosome 6A.

Using markers *GENE-4021_496*, *AX-95182345* and *AX-94634087* for haplotype construction resulted in the three distinct haplotypes CGT, TAG and CAT. Details of them are listed in Table 2. The CGT haplotype was by far the most common, followed by TAG, while the CAT haplotype was rare, only found in 3 and 2 of the tested lines in 2013 and 2014, respectively (Table 2).

The haplotype effects of the two most common haplotype groups were studied further. This revealed highly consistent haplotype effects with the CGT allele always being associated with a significantly lower chlorosis level than the TAG haplotype,

Table 2 Haplotypes constructed using 25 K markers *GENE-4021_496*, *AX-95182345* and *AX-94634087* along with number of lines assigned to each haplotype in different years of testing

Year	Haplotype Numbering	Haplotype	Number of lines per haplotype
2013	1	TAG	19
	2	CAT	3
	3	CGT	112
2014	1	TAG	20
	2	CAT	2
	3	CGT	95

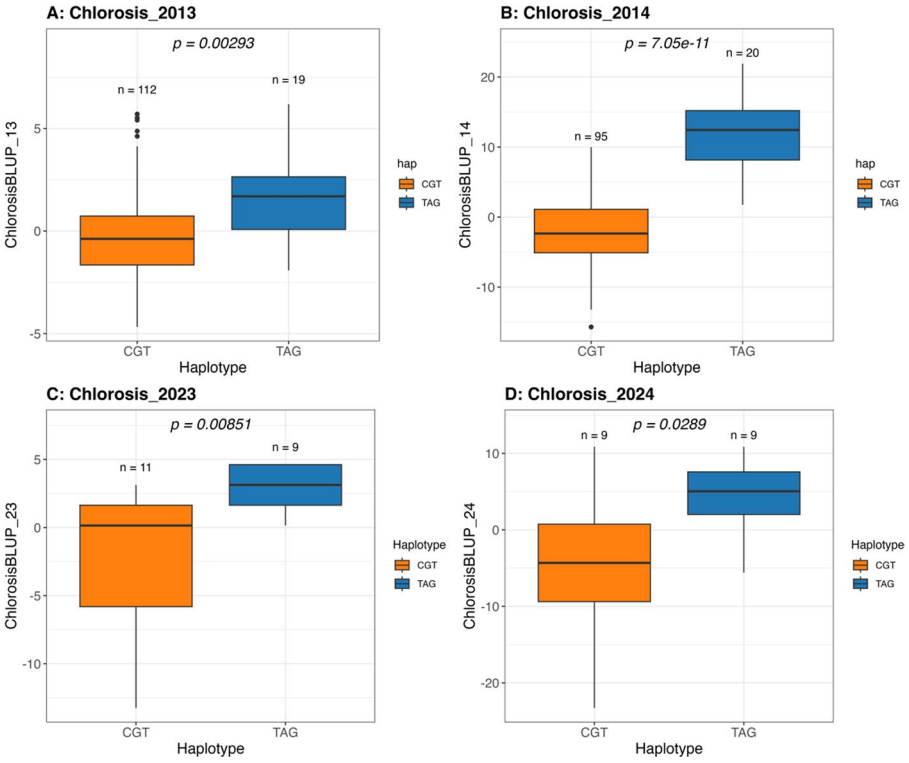

Fig. 6 Box plot showing the phenotypic differences for mean chlorosis in spring wheat panel 2013 (**A**) and 2014 (**B**), twenty MASBASIS lines in 2023 greenhouse trial (**C**) and eighteen RILs derived from GN07560 × Seniorita in 2024 (**D**) of two major haplotype groups of QWl.nmbu-6A constructed by the 25 K SNP markers *GENE-4021_496*, *AX-95182345* and *AX-94634087* with number of lines per haplotypes denoted by n in top of each boxplot. The results of Welch's two-sample t test (p-value) between the two contrasting haplotype groups are shown on the top of each diagram

both for the field trials in 2013 and 2014 and the two greenhouse tests using selected MASBASIS lines and segregating RILs from the cross between GN07560 and Seniorita (Fig. 6). The QTL explains 7% of the variation for chlorosis in experimental year 2013 while 54% of the phenotypic variation in experimental year 2014 (see supplementary Fig. S6). Across years, the QTL accounted for 30.75% of the phenotypic variance ($P = 6.28 \times 10^{-27}$) (see supplementary Fig. S6 and Table S2).

Discussion

In this study, we reanalyzed data from Sundgren et al. (2018) using updated GWAS models and further evaluated the major QTL, *QWl.nmbu-6A*, through additional greenhouse experiments. Phenotypic traits recorded in both field years included chlorosis percentage, relative plant height, heading delay, and overall condition score. As reported by Sundgren et al. (2018), Pearson correlation analysis showed that all traits except overall condition score were positively correlated between 2013 and

2014, with most correlations around 0.3 (Fig. 2). In contrast, overall condition score exhibited little to no consistency across years. Because waterlogging tolerance is highly influenced by environmental variation (Herzog et al. 2016; McDonald et al. 2006; Setter et al. 2009), the differing trait responses between the two seasons were likely associated with differences in weather conditions and stress intensity. The 2013 season was cooler and wetter than the 2014 season, and waterlogging was imposed for 10 days in 2013 and 13 days in 2014. The longer treatment in 2014 was used to intensify the stress and produced more clearly differentiated chlorotic symptoms among genotypes. It also delayed plant development, as reflected by heading delay, and more strongly affected overall condition near maturity (Sundgren et al. 2018).

Many traits are affected by waterlogging, and there is no precise consensus on a specific trait to be used as selection criterion for waterlogging tolerance. So, the phenotyping approach that was used by Sundgren et al. (2018) was to record all the affected traits that are easily quantified. To remove potential noise while also retaining the relevant information from the data, PCA was used. PC1 scores were used to rank the genotypes' overall performances rather than considering single trait as criterion to determine sensitive and tolerant genotypes. PCA utilizes the dimensionality-reduction method through which it transforms multiple correlated phenotypes into smaller sets of uncorrelated variables known as principal components (PCs), that can capture the major patterns in the datasets (He et al. 2008; Zhang et al. 2023). GWAS and PCA are a good combination when analyzing phenotypically complex traits and this approach has been validated as effective in detecting causal genes related to complex traits (Yano et al. 2019). In the present study, PCA results indicated that in 2013, PC1 was influenced by overall condition, heading delay, and chlorosis, whereas chlorosis-related variation was also distributed across PC2 and PC3. Notably, PC2, although primarily driven by plant height, showed a substantial contribution from chlorosis, and the significant association of the *QWl.nmbu-6A* with PC2 in the GWAS result indicates that the genetic signal is linked to this structured component of chlorosis variation rather than the variation represented by PC1. In contrast, in 2014, the inclusion of recovery-related traits, particularly green biomass, resulted in a clearer partitioning of variation, with PC1 primarily reflecting recovery traits and showing minimal contribution from chlorosis, while chlorosis contributed more distinctly to PC2 and PC3. *QWl.nmbu-6A* was distinctly observed in PC2 and PC3 in 2014, further supporting its association with foliar chlorosis-related variation captured in these components. This shift indicates that foliar chlorosis captures variation largely independent of recovery-related traits and that its genetic effects are more effectively resolved in components less influenced by recovery processes.

The differences observed between years in the PCA were also reflected in the heritability estimates for foliar chlorosis. Broad-sense heritability was 0.59 in 2013 and 0.87 in 2014 but decreased to 0.40 in the combined analysis across years. Genotype × year variance was not included in the individual-year analyses because each analysis contained only one year. In contrast, the combined analysis included both years and incorporated variation between environments, including genotype-specific differences in responses across years. The lower across-year heritability therefore indicates that the relative chlorosis responses of the genotypes were not fully consistent between environments.

The phenotypic variance in chlorosis explained by *QWl.nmbu-6A* also differed markedly between years, increasing from 7.3% in 2013 to 54.1% in 2014, with an across-year estimate of 30.8%. The longer waterlogging treatment in 2014 produced stronger and more clearly differentiated chlorotic symptoms, increasing the phenotypic contrast between haplotype groups and potentially increasing the estimated contribution of the locus. Conversely, the shorter treatment and greater environmental or residual variation in 2013 may have reduced the detectable effect of the QTL. Differences in temperature, rainfall, soil redox conditions, plant development, and spatial heterogeneity may also have contributed to genotype-specific responses. The intermediate across-year estimate reflects the QTL effect across the two contrasting environments while incorporating genotype × year variation. These differences also support environmentally dependent expression of *QWl.nmbu-6A*.

Waterlogging tolerance is a complex quantitative trait that is strongly affected by environmental conditions (Ding et al. 2023). In different mapping populations, QTL controlling waterlogging-related traits in wheat have been mapped to numerous genomic regions. *QWl.nmbu-6A*, located at approximately 610–613 Mb on chromosome 6A, was the most consistent region associated with chlorotic symptoms in waterlogged plants in the present analyses. The supplementary GWAS analyses were treated as sensitivity analyses. In 2014, *GENE-4021_496* at 610.35 Mb exceeded the Bonferroni threshold in all nine combinations of the BLINK, FarmCPU, and MLM models fitted with zero, one, or two principal components. The chromosome 6 A region was also detected for chlorosis-related PC2 and PC3 phenotypes, providing additional support for its association with foliar chlorosis.

Importantly, *GENE-4021_496* remained significant in all nine corresponding analyses after the exotic germplasm was excluded and only the adapted lines were analyzed. In contrast, most other associations were detected in only one model, principal-component setting, or germplasm subset (see Supplementary material, Table S6 and S7). Thus, *QWl.nmbu-6A* was the most analytically stable chlorosis-associated region in 2014, and its detection was not solely attributable to model choice, the number of principal components used to correct for population structure, or differences between adapted and exotic germplasm. This analytical consistency strengthens confidence in the association and reason to further validate this region.

To further evaluate the chromosome 6A region, haplotypes were constructed using the most significant marker, *GENE-4021_496*, together with *AX-95182345* and *AX-94634087*, which were in strong linkage disequilibrium with the lead marker. The pairwise LD values between *GENE-4021_496* and *AX-95182345* and between *GENE-4021_496* and *AX-94634087* were $R^2 = 0.94$ and $R^2 = 0.85$, respectively. These three markers defined the major CGT and TAG haplotypes used to evaluate the phenotypic effect of *QWl.nmbu-6A*. Welch's two-sample t-tests showed that mean chlorosis percentage, expressed as BLUPs, differed significantly between the two contrasting haplotype groups in both 2013 and 2014. Lines carrying the CGT haplotype were significantly less chlorotic than those carrying the TAG haplotype.

Although the haplotype groups differed significantly in both years, the strength of the corresponding single-marker GWAS evidence varied substantially. In 2013, *GENE-4021_496*, *AX-95182345*, and *AX-94634087* did not reach the exploratory threshold of $-\log_{10}(P) = 3$, and no marker for foliar chlorosis exceeded the Bonferroni

threshold. In contrast, *GENE-4021_496* exceeded the Bonferroni threshold across all GWAS models and PC counts in 2014. The lower heritability and greater environmental or residual variation in 2013 likely reduced the statistical power of the single-marker analysis, making it more difficult for individual markers to exceed the genome-wide threshold. Conversely, the higher heritability and stronger phenotypic differentiation in 2014 increased the signal relative to environmental variation and improved the power to detect the locus.The absence of a genome-wide significant single-marker association in 2013 was, however, not interpreted as evidence that *QWl.nmbu-6A* had no effect that year. The GWAS and haplotype analyses tested related but different hypotheses. The GWAS evaluated individual markers under a stringent genome-wide multiple-testing correction, whereas the targeted haplotype analysis compared two predefined groups using three markers in strong LD. The haplotype may have represented regional variation more effectively, and the targeted comparison involved a much smaller multiple-testing burden. Thus, the significant haplotype difference in 2013 was consistent with the absence of a significant genome-wide individual marker. Rather, the difference between years was primarily quantitative, reflecting variation in the magnitude and statistical detectability of the association.

Several QTL associated with waterlogging or flooding responses have previously been reported on chromosome 6A (Burgos et al. 2001; Yu and Chen 2013). Burgos et al. (2001) identified chromosome 6A QTL associated with seedling growth and germination-related responses following flooding in the Forno × Oberkulmer wheat–spelt RIL population. The reported support intervals were defined using the original genetic map and cannot be projected unambiguously onto IWGSC RefSeq v2.1 because physical coordinates are unavailable for the delimiting markers. Consequently, their physical relationship to *QWl.nmbu-6A* remains unresolved. Yu and Chen (2013) identified two chromosome 6 A intervals, *Xpsr10–Xfba85* and *Xcdo772–Xfbb170*, associated with waterlogging-related root, shoot and total dry-weight indices in the W7984 × Opata85 ITMI RIL population. The *Xpsr10–Xfba85* interval has historical marker evidence placing it on chromosome arm 6AS. The Wheat Gene Catalogue lists *Xfba85-6A* and *Xpsr10(Gli-2)-6A* as markers associated with the winter-hardiness QTL *QWin.ipk-6A* on 6AS (McIntosh 2024). Erayman et al. (2004) also listed both markers in the homoeologous group-6 consensus gene-rich region 6S1.0, which includes 6AS deletion lines. At the chromosome-arm level, this interval is therefore distinct from *QWl.nmbu-6A* on 6AL. The Xcdo772–Xfbb170 interval has historical evidence placing it on 6AL. In the integrated chromosome 6A linkage map of Shi et al. (2003), which incorporated previously mapped markers from GrainGenes, Xcdo772-6A and Xfbb170-6A were positioned at approximately 64.1 and 69.2 cM, respectively. Erayman et al. (2004) also listed the corresponding markers in the homoeologous group-6 consensus gene-rich regions 6L0.4 and 6L0.9, respectively, both of which include chromosome 6AL deletion lines. However, validated probe sequences and unambiguous IWGSC RefSeq v2.1 coordinates are not currently available. Consequently, this historical interval cannot be converted reliably into a sequence-based physical interval, and its overlap with *QWl.nmbu-6A* at Chr6A:610–613 Mb cannot presently be confirmed. A broader screening of published wheat waterlogging studies also did not identify another physically anchored waterlogging QTL overlapping the *QWl.nmbu-6A* interval at Chr6A:610–613 Mbp. More

recent studies identified germination-stage waterlogging QTL on chromosomes 5A, 7B and 2D (Pang et al. 2022), root-survival and aerenchyma associations on chromosomes 2A, 2D, 4A, 4B, 5A, 5B, 7A and 7D (Xu et al. 2022), and stable post-anthesis waterlogging QTL on chromosomes 4AL, 5AS and 7DL (Ding et al. 2023). Similarly, a recent waterlogging-tolerance locus derived from synthetic hexaploid wheat was reported on chromosome 1D rather than 6A (Cao et al. 2026). The multi-stress meta-analysis of Tanin et al. (2022) also did not identify a chromosome 6A meta-QTL derived from waterlogging studies; its chromosome 6 A meta-QTL were associated with other abiotic stresses. Therefore, the currently available literature provides no evidence for another physically anchored wheat waterlogging QTL overlapping Chr 6A:610–613 Mb. Thus, *QWl.nmbu-6A* (610–613 Mb) identified in this study represents a putatively novel genomic region associated with chlorosis under waterlogging stress in wheat. To the best of our knowledge, no QTL has previously been reported for this region on chromosome 6A for foliar chlorosis under waterlogging in wheat.

QWl.nmbu-6A was further evaluated through greenhouse waterlogging experiments. Significant differences in mean chlorosis percentage were observed between the two haplotype groups in selected MASBASIS genotypes and GN07560 × Seniorita RILs subjected to starch-induced waterlogging stress. Notably, a significant haplotype effect was detected only when severe stress conditions were created using a starch solution. Although waterlogging with pure water created a reduced soil environment, a haplotype effect was not detected under the milder pure-water treatment or control conditions (Khadka 2023). Replication of the haplotype effect in a biparental background reduces potential confounding from the broad population structure of the diversity panel and provides additional evidence that *QWl.nmbu-6A* is associated with severe waterlogging-induced chlorosis. However, because interval recombinants were not represented in the selected greenhouse subset, these experiments validate a haplotype-region effect but do not fine-map the causal locus.

Sundgren et al. (2018) also conducted yield-registration experiments in 2015 and 2016 to determine the relevance of foliar chlorosis and PC1 under field conditions. Foliar chlorosis was significantly negatively correlated with overall condition at maturity in both 2015 ($r = -0.79$, $P = 0.003$) and 2016 ($r = -0.62$, $P = 0.01$). Under the more severe stress conditions in 2015, chlorosis explained 87% of the variation in relative grain yield (adjusted $R^2 = 0.87$, $p < 0.001$), supporting its value as a proxy trait when chlorotic injury is strongly expressed. Its ability to predict relative grain yield was weaker under the milder conditions in 2016 (Sundgren et al. 2018). The 2014 PCA and Pearson correlation results further showed that green biomass had the strongest influence on PC1 and was positively correlated with overall condition. Green biomass reflected recovery at an earlier developmental stage, whereas overall condition was evaluated closer to maturity. These findings show that chlorosis percentage may not always correlate strongly with the final condition of plants and are consistent with Setter and Waters (2003). Measurements of recovery should therefore be included in assessments of waterlogging tolerance (Sundgren 2018).

Foliar chlorosis was treated in this study as an early proxy for waterlogging-induced injury rather than as a direct or complete measure of waterlogging tolerance. It is readily visible, can be assessed within a relatively short period, and effectively differentiates genotypes under sufficiently severe stress. Nevertheless, it does not

fully represent root adaptation, anaerobic metabolism, survival, post-stress recovery, biomass retention, spike fertility, or grain yield. Its expression may also be influenced by stress intensity and duration, developmental stage, temperature, soil conditions and assessment time. Accordingly, *QWl.nmbu-6A* is interpreted specifically as a marker-defined region associated with foliar chlorosis under waterlogging. Its biological specificity is supported by its association with chlorosis and chlorosis-related principal components, but the physiological or molecular mechanism underlying this association remains unresolved.

Our findings highlight the complex, stress-dependent nature of chlorosis expression under waterlogging stress and validate the association between *QWl.nmbu-6A* and this trait. Together, the cross-model and cross-subset consistency, strong LD among the selected markers, significant field haplotype effects, and replication under severe greenhouse waterlogging support the relevance of *QWl.nmbu-6A*. Notably, foliar chlorosis emerged as a critical early stress indicator, with its predictive power for overall plant performance and yield differences depending on stress intensity and environmental conditions. The observation that chlorosis is associated with PC2 and PC3 rather than PC1 in 2014 further suggests that chlorosis reflects an early-stage stress response mechanism, likely under distinct genetic control from the recovery traits influencing biomass and yield, which were more aligned with PC1. Detection of *QWl.nmbu-6A* with chlorosis and chlorosis-driven PCs (PC2 and PC3) across environments and GWAS models emphasizes the relevance of this QTL. Since *QWl.nmbu-6A* is specific to chlorosis and chlorosis does not always correlate strongly with recovery traits or final yield under mild stress, relying solely on this QTL might miss genotypes that recover well despite showing early chlorotic symptoms. These results also indicate potential breeding utility, particularly in environments prone to moderate to severe waterlogging where the QTL effect is fully expressed. However, the magnitude and statistical detectability of the QTL effect varied across years and stress treatments. The breeding value of *QWl.nmbu-6A* should therefore be evaluated across additional years, locations, genetic backgrounds, and waterlogging intensities. Fine mapping using informative recombinants, denser genotyping or sequencing, and near-isogenic material will also be required to reduce the marker-defined interval and identify the underlying causal gene or genes. Until such validation is completed, *QWl.nmbu-6A* should be used as a promising marker-defined region for severe waterlogging-induced chlorosis and combine with complementary phenotypic assessments and markers for recovery and agronomic performance.

Chlorosis, a visible stress symptom, varies significantly among genotypes and may be linked to root characteristics prior to waterlogging. Interestingly, other large-effect QTL have been identified in the same genomic region of chromosome 6A, such as *QRGA.UBO-6A.2* (Maccaferri et al. 2016), *qSRA-6A* (Alahmad et al. 2019), and *EPdwRGA-6A* (Alemu et al. 2021), significantly associated with seminal root angle in different durum wheat populations. Since foliar chlorosis primarily reflects root-level stress responses, the overlapping genomic region suggests that *QWl.nmbu-6A* associated with chlorosis under waterlogging may also be linked to variation in seminal root angle. Further studies exploring this potential association would be valuable to determine whether genes controlling chlorosis are related to those influencing seminal root angle.

Conclusion

The QTL *QWl.nmbu-6A*, located within the 610–613 Mbp region on chromosome 6 A was the important QTL associated with foliar chlorosis under waterlogging stress found from this study. We also successfully validated this QTL in greenhouse conditions. Foliar chlorosis emerged as a valuable early indicator of waterlogging sensitivity, particularly under severe stress, though its predictive value decreased under milder conditions. Findings on this study also emphasize that waterlogging tolerance is a complex, environment-dependent trait, where both early stress responses and recovery traits must be considered. The tightly linked markers to *QWl.nmbu-6A* offer a promising tool for marker-assisted selection (MAS) in breeding programs. However, complementary selection strategies incorporating recovery traits are essential. Future research should focus on elucidating proxy root traits contributing to tolerance during waterlogging stress, exploring the genetic mechanisms underlying root and shoot responses, and unraveling the molecular and biochemical pathways involved in oxygen sensing and reactive oxygen species (ROS) detoxification. Such studies will further strengthen breeding efforts for improved waterlogging tolerance in wheat.

Supplementary Information The online version contains supplementary material available at https://doi.org/10.1007/s11032-026-01742-w.

Acknowledgements This work was funded by The Research Council of Norway (the BIONAER program) through the AGROPRO project (NFR project no. 225330). AK and AKR were funded through the SproutResist project "Genomic-based breeding technology for the improvement of pre-harvest sprouting resistance in wheat under Norwegian climate" (NFR project no. 321436) . We thank Svend Pung and Jens Andreas Randem at the Centre for Plant Research in Controlled Environment (SKP) for technical support with the field experiments. The authors want to thank Anne Kjersti Uhlen at NMBU for her contribution to the initial work, including project planning, funding acquisition and supervision of the work. Open access funding was provided by the Norwegian University of Life Sciences.

Authors' contributions AK wrote the manuscript, did the final data analysis, designed and conducted the greenhouse experiments. AKR supervised the greenhouse experiments and data analysis, edited the manuscript. TKS designed and conducted the waterlogging field trials, did statistical analysis of the field trial phenotypes, did the initial GWAS analysis, commented on and edited the manuscript.TB conducted filtering and analysis of the original 35 K SNP chip data, initial GWAS, commented on and edited the manuscript. ML ield trials, contributed to the original concept, obtained funding, supervised the work done by TKS and AK. All coauthors have read and approved the final version of the manuscript.

Funding Open access funding provided by Norwegian University of Life Sciences. This work was funded by The Research Council of Norway (the BIONAER program) through the AGROPRO project (NFR project no. 225330). AK and AKR were funded through the SproutResist project "Genomic-based breeding technology for the improvement of pre-harvest sprouting resistance in wheat under Norwegian climate" (NFR project no. 321436).

Data availability Data generated and analyzed for this study is included as supporting material for this submission and will be made publicly available upon publication. Phenotypic data from the field trials have been published before and is available from Sundgren et al. (2018). Breeding lines are anonymized.

Declarations

Clinical trial number Not applicable.

Competing interests One of the authors, Prof. Morten Lillemo, is on the editorial board of this special issue (Genome-informed Wheat Breeding for End-use Quality, Pathogen Invasion and Resilience to Climate Extremes) of Molecular Breeding, and has co-authored papers with editors He Zhonghu and Xia Xianchun. For consideration of our manuscript, we suggest Dr. Yuanfeng Hao as editor. TKS is employed at Yara Suomi Oy.

Open Access This article is licensed under a Creative Commons Attribution 4.0 International License, which permits use, sharing, adaptation, distribution and reproduction in any medium or format, as long as you give appropriate credit to the original author(s) and the source, provide a link to the Creative Commons licence, and indicate if changes were made. The images or other third party material in this article are included in the article's Creative Commons licence, unless indicated otherwise in a credit line to the material. If material is not included in the article's Creative Commons licence and your intended use is not permitted by statutory regulation or exceeds the permitted use, you will need to obtain permission directly from the copyright holder. To view a copy of this licence, visit http://creativecommons.org/licenses/by/4.0/.

References

Alahmad S, El Hassouni K, Bassi FM, Dinglasan E, Youssef C, Quarry G, Aksoy A, Mazzucotelli E, Juhász A, Able JA, Christopher J, Voss-Fels KP, Hickey LT (2019) A major root architecture QTL responding to water limitation in durum wheat. Front Plant Sci 10:436. https://doi.org/10.3389/fpls.2019.00436

Alemu A, Feyissa T, Maccaferri M, Sciara G, Tuberosa R, Ammar K, Badebo A, Acevedo M, Letta T, Abeyo B (2021) Genome-wide association analysis unveils novel QTLs for seminal root system architecture traits in Ethiopian durum wheat. BMC Genomics 22:20. https://doi.org/10.1186/s12864-020-07320-4

Arduini I, Orlandi C, Pampana S, Masoni A (2016) Waterlogging at tillering affects spike and spikelet formation in wheat. Crop Pasture Sci 67:703–711. https://doi.org/10.1071/CP15417

Ballesteros DC, Mason RE, Addison CK, Acuña MA, Arguello MN, Subramanian N, Miller RG, Sater H, Gbur EE, Miller D et al (2015) Tolerance of wheat to vegetative stage soil waterlogging is conditioned by both constitutive and adaptive QTL. Euphytica 201:329–343. https://doi.org/10.1007/s10681-014-1184-3

Boden SA, McIntosh RA, Uauy C, Krattinger SG, Dubcovsky J, Rogers WJ, Xia XC, Badaeva ED, Bentley AR, Brown-Guedira G et al (2023) Updated guidelines for gene nomenclature in wheat. Theor Appl Genet 136:72. https://doi.org/10.1007/s00122-023-04253-w

Bradbury PJ, Zhang Z, Kroon DE, Casstevens TM, Ramdoss Y, Buckler ES (2007) TASSEL: software for association mapping of complex traits in diverse samples. Bioinformatics 23:2633–2635. https://doi.org/10.1093/bioinformatics/btm308

Breseghello F, Sorrells ME (2006) Association analysis as a strategy for improvement of quantitative traits in plants. Crop Sci 46:1323–1330. https://doi.org/10.2135/cropsci2005.09-0305

Byrne T, Grant J, Kock-Appelgren P, Förster L, Michel T, Miricescu A, Thomas WTB, Graciet E, Spink J, Ng CKY et al (2022) Improving phenotyping in winter barley cultivars towards waterlogging tolerance by combining field trials under natural conditions with controlled growth condition experiments. Eur J Agron 133:126432. https://doi.org/10.1016/j.eja.2021.126432

Cao D, Hao M, Liang Y, Gong Z, Gan X, Li Y, Liu D, Liu B (2026) A reference assembly for the D-subgenome parent resolves introgression and waterlogging tolerance loci in synthetic hexaploid wheat. Crop J. https://doi.org/10.1016/j.cj.2026.07.001

Collaku A, Harrison S (2002) Losses in wheat due to waterlogging. Crop Sci 42:444–450. https://doi.org/10.2135/cropsci2002.4440

Ding J, Liang P, Wu P, Zhu M, Li C, Zhu X, Gao D, Chen Y, Guo W (2020) Effects of waterlogging on grain yield and associated traits of historic wheat cultivars in the middle and lower reaches of the Yangtze River, China. Field Crops Res 246:107695. https://doi.org/10.1016/j.fcr.2019.107695

Ding F, Tong J, Xu R, Chen J, Xu X, Nadeem M, Wang S, Zhang Y, Zhu Z, Wang F et al (2023) Identification of stable quantitative trait loci underlying waterlogging tolerance post-anthesis in common wheat (Triticum aestivum). Crop J 11:1163–1170. https://doi.org/10.1016/j.cj.2023.06.004

Endelman JB (2011) Ridge regression and other kernels for genomic selection with R package rrBLUP. Plant Genome 4:250–255. https://doi.org/10.3835/plantgenome2011.08.0024
Erayman M, Sandhu D, Sidhu D, Dilbirligi M, Baenziger PS, Gill KS (2004) Demarcating the gene-rich regions of the wheat genome. Nucleic Acids Res 32:3546–3565. https://doi.org/10.1093/nar/gkh639
Feyen L, Dankers R, Bódis K, Salamon P, Barredo JI (2012) Fluvial flood risk in Europe in present and future climates. Clim Change 112:47–62. https://doi.org/10.1007/s10584-011-0339-7
Flint-Garcia SA, Thornsberry JM, Buckler ESIV (2003) Structure of linkage disequilibrium in plants. Annu Rev Plant Biol 54:357–374. https://doi.org/10.1146/annurev.arplant.54.031902.134907
Gardner W, Flood R (1993) Less waterlogging damage with long season wheats. Cereal Res Commun 21:337–343. https://www.jstor.org/stable/23783988
Greenway H, Armstrong W, Colmer TD (2006) Conditions leading to high CO2 (> 5 kPa) in waterlogged–flooded soils and possible effects on root growth and metabolism. Ann Botany 98:9–32. https://doi.org/10.1093/aob/mcl076
Gupta PK, Kulwal PL, Jaiswal V (2014) Association mapping in crop plants: opportunities and challenges. Adv Genet 85:109–147. https://doi.org/10.1016/B978-0-12-800271-1.00002-0
Hamazaki K, Iwata H (2020) RAINBOW: Haplotype-based genome-wide association study using a novel SNP-set method. PLoS Comput Biol 16:e1007663. https://doi.org/10.1371/journal.pcbi.1007663
He LN, Liu YJ, Xiao P, Zhang L, Guo Y, Yang TL, Zhao LJ, Drees B, Hamilton J, Deng HY et al (2008) Genomewide linkage scan for combined obesity phenotypes using principal component analysis. Ann Hum Genet 72:319–326. https://doi.org/10.1111/j.1469-1809.2007.00423.x
Herzog M, Striker GG, Colmer TD, Pedersen O (2016) Mechanisms of waterlogging tolerance in wheat–a review of root and shoot physiology. Plant Cell Environ 39:1068–1086. https://doi.org/10.1111/pce.12676
Hickey LT, Hafeez AN, Robinson H, Jackson SA, Leal-Bertioli SCM, Tester M, Gao C, Godwin ID, Hayes BJ, Wulff BBH (2019) Breeding crops to feed 10 billion. Nat Biotechnol 37:744–754. https://doi.org/10.1038/s41587-019-0152-9
Huang M, Liu X, Zhou Y, Summers RM, Zhang Z (2019) BLINK: a package for the next level of genome-wide association studies with both individuals and markers in the millions. GigaScience 8:giy154. https://doi.org/10.1093/gigascience/giy154
Husson O (2013) Redox potential (Eh) and pH as drivers of soil/plant/microorganism systems: a transdisciplinary overview pointing to integrative opportunities for agronomy. Plant Soil 362:389–417. https://doi.org/10.1007/s11104-012-1429-7
Ingvarsson PK, Street NR (2011) Association genetics of complex traits in plants. New Phytol 189:909–922. https://doi.org/10.1111/j.1469-8137.2010.03593.x
Kaur G, Singh G, Motavalli PP, Nelson KA, Orlowski JM, Golden BR (2020) Impacts and management strategies for crop production in waterlogged or flooded soils: A review. Agron J 112:1475–1501. https://doi.org/10.1002/agj2.20093
Khabaz-Saberi H, Barker S, Rengel Z (2012) Tolerance to ion toxicities enhances wheat (Triticum aestivum L.) grain yield in waterlogged acidic soils. Plant Soil 354:371–381. https://doi.org/10.1007/s11104-011-1073-7
Khadka A (2023) *Optimization of greenhouse waterlogging tolerance screening and low-cost seminal root phenotyping methods for spring wheat*. Master's thesis, Norwegian University of Life Sciences. https://hdl.handle.net/11250/3097344
Korte A, Farlow A (2013) The advantages and limitations of trait analysis with GWAS: a review. Plant Methods 9:29. https://doi.org/10.1186/1746-4811-9-29
Li H, Vaillancourt R, Mendham N, Zhou M (2008) Comparative mapping of quantitative trait loci associated with waterlogging tolerance in barley (Hordeum vulgare L). BMC Genomics 9:401. https://doi.org/10.1186/1471-2164-9-401
Lin M, Dieseth JA, Alsheikh M, Yang E, Holzapfel J, Schürmann F, Morales L, Michel S, Buerstmayr H, Bhavani S, Lillemo M (2023) A major yellow rust resistance QTL on chromosome 6A shows increased frequency in recent Norwegian spring wheat cultivars and breeding lines. Theor Appl Genet 136:164. https://doi.org/10.1007/s00122-023-04397-9
Lipka AE, Tian F, Wang Q, Peiffer J, Li M, Bradbury PJ, Gore MA, Buckler ES, Zhang Z (2012) GAPIT: genome association and prediction integrated tool. Bioinformatics 28:2397–2399. https://doi.org/10.1093/bioinformatics/bts444
Liu X, Huang M, Fan B, Buckler ES, Zhang Z (2016) Iterative usage of fixed and random effect models for powerful and efficient genome-wide association studies. PLoS Genet 12:e1005767. https://doi.org/10.1371/journal.pgen.1005767

Maccaferri M, El-Feki W, Nazemi G, Salvi S, Canè MA, Colalongo MC, Stefanelli S, Tuberosa R (2016) Prioritizing quantitative trait loci for root system architecture in tetraploid wheat. J Exp Bot 67:1161–1178. https://doi.org/10.1093/jxb/erw039

Macías F, Camps Arbestain M (2010) Soil carbon sequestration in a changing global environment. Mitig Adapt Strat Glob Change 15:511–529. https://doi.org/10.1007/s11027-010-9231-4

McIntosh RA (2024) Catalogue of gene symbols for wheat: 2024 edition (covering all WGC curations). GrainGenes. https://graingenes.org/GG3/Wheat_Gene_Catalog_Documents. https://graingenes.org/GG3/Wheat_Gene_Catalog_Documents. Accessed 13 Nov 2026

Mano Y, Takeda K (2012) Accurate evaluation and verification of varietal ranking for flooding tolerance at the seedling stage in barley (Hordeum vulgare L). Breed Sci 62:3–10. https://doi.org/10.1270/jsbbs.62.3

Masson-Delmotte V, Zhai P, Pirani A, Connors SL, Péan C, Berger S, Caud N, Chen Y, Goldfarb L, Gomis MI et al (eds) (2021) Climate change 2021: the physical science basis. *Contribution of Working Group I to the Sixth Assessment Report of the Intergovernmental Panel on Climate Change*. Cambridge University Press, Cambridge. https://doi.org/10.1017/9781009157896

McDonald G, Setter T, Waters I, Tugwell R (2006) Screening for waterlogging tolerance of wheat in the field in Western Australia. Proceedings of the 13th Australian Society of Agronomy Conference, Perth, Western Australia

Mfarrej M, Wang X, Hamzah Saleem M, Hussain I, Rasheed R, Arslan Ashraf M, Iqbal M, Sohaib Chattha M, Nasser Alyemeni M (2022) Hydrogen sulphide and nitric oxide mitigate the negative impacts of waterlogging stress on wheat (Triticum aestivum L). Plant Biol 24:670–683. https://doi.org/10.1111/plb.13358

Musgrave M, Ding N (1998) Evaluating wheat cultivars for waterlogging tolerance. Crop Sci 38:90–97. https://doi.org/10.2135/CROPSCI1998.0011183X003800010016X

Nickum MT, Crane J, Schaffer B, Davies FS (2011) Leaf net CO2 assimilation, electrolyte leakage, and alcohol dehydrogenase activity in roots of mamey sapote (Pouteria sapota) trees as affected by root-zone oxygen content. Proc Fla State Hortic Soc 124:18–22

Olgun M, Metin Kumlay A, Cemal Adiguzel M, Caglar A (2008) The effect of waterlogging in wheat (T. aestivum L). Acta Agriculturae Scand Sect B — Soil Plant Sci 58:193–198. https://doi.org/10.1080/09064710701794024

Pampana S, Masoni A, Arduini I (2016) Grain yield of durum wheat as affected by waterlogging at tillering. Cereal Res Commun 44:706–716. https://doi.org/10.1556/0806.44.2016.026

Pang J, Zhou M, Mendham N, Shabala S (2004) Growth and physiological responses of six barley genotypes to waterlogging and subsequent recovery. Aust J Agric Res 55:895–906. https://doi.org/10.1071/AR03097

Pang Y, Wang X, Zhao M, Lu Y, Yan Q, Sun S, Wang Y, Liu S (2022) Identification and validation of the genomic regions for waterlogging tolerance at germination stage in wheat. Agronomy 12:1848. https://doi.org/10.3390/agronomy12081848

Ploschuk RA, Miralles DJ, Striker GG (2021) Early- and late-waterlogging differentially affect the yield of wheat, barley, oilseed rape and field pea through changes in leaf area index, radiation interception and radiation use efficiency. J Agron Crop Sci 207:504–520. https://doi.org/10.1111/jac.12486

Purcell S, Neale B, Todd-Brown K, Thomas L, Ferreira MAR, Bender D, Maller J, Sklar P, de Bakker PIW, Daly MJ et al (2007) PLINK: a tool set for whole-genome association and population-based linkage analyses. Am J Hum Genet 81:559–575. https://doi.org/10.1086/519795

Sandhu KS, Burke AB, Merrick LF, Pumphrey MO, Carter AH (2024) Comparing performances of different statistical models and multiple threshold methods in a nested association mapping population of wheat. Front Plant Sci 15:1460353. https://doi.org/10.3389/fpls.2024.1460353

Setter T, Waters I (2003) Review of prospects for germplasm improvement for waterlogging tolerance in wheat, barley and oats. Plant Soil 253:1–34. https://doi.org/10.1023/A:1024573305997

Setter T, Burgess P, Waters I, Kuo J (1999) Genetic diversity of barley and wheat for waterlogging tolerance in Western Australia. Proceedings of the 9th Australian Barley Technical Symposium, Melbourne, Victoria, Australia

Setter TL, Waters I, Sharma SK, Singh KN, Kulshreshtha N, Yaduvanshi NPS, Ram PC, Singh BN, Rane J, McDonald G et al (2009) Review of wheat improvement for waterlogging tolerance in Australia and India: the importance of anaerobiosis and element toxicities associated with different soils. Ann Botany 103:221–235. https://doi.org/10.1093/aob/mcn137

Shi JR, Song QJ, Singh S, Lewis J, Ward RW, Cregan P, Gill BS (2003) Genetic and physical maps of Xbarc SSR loci in wheat. In: Canty SM, Lewis J, Ward RW (eds) Proceedings of the 2003 National Fusarium Head Blight Forum, Bloomington, Minnesota, USA, 13–15 December 2003. Michigan State University, East Lansing, pp 41–45. https://scabusa.org/pdfs/forum_03_proc.pdf. Accessed 13 Nov 2026

St. Burgos M, Messmer MM, Stamp P, Schmid JE (2001) Flooding tolerance of spelt (Triticum spelta L.) compared to wheat (Triticum aestivum L.): a physiological and genetic approach. Euphytica 122:287–295. https://doi.org/10.1023/A:1012945902299

Sundgren TK (2018) *Phenotypic and genetic studies of waterlogging tolerance in wheat and barley*. Doctoral thesis, Norwegian University of Life Sciences. https://hdl.handle.net/11250/2577081

Sundgren TK, Uhlen AK, Waalen W, Lillemo M (2018) Field screening of waterlogging tolerance in spring wheat and spring barley. Agronomy 8:38. https://doi.org/10.3390/agronomy8040038

Tadesse W, Sanchez-Garcia M, Assefa SG, Amri A, Bishaw Z, Ogbonnaya FC, Baum M (2019) Genetic gains in wheat breeding and its role in feeding the world. Crop Breed Genet Genomics 1(1). https://doi.org/10.20900/cbgg20190005

Tanin MJ, Saini DK, Sandhu KS, Pal N, Gudi S, Chaudhary J, Sharma A (2022) Consensus genomic regions associated with multiple abiotic stress tolerance in wheat and implications for wheat breeding. Sci Rep 12:13680. https://doi.org/10.1038/s41598-022-18149-0

Wang J, Zhang Z (2021) GAPIT version 3: boosting power and accuracy for genomic association and prediction. Genom Proteom Bioinform 19:629–640. https://doi.org/10.1016/j.gpb.2021.08.005

Xu L, Zhao C, Pang J, Niu Y, Liu H, Zhang W, Zhou M (2022) Genome-wide association study reveals quantitative trait loci for waterlogging-triggered adventitious roots and aerenchyma formation in common wheat. Front Plant Sci 13:1066752. https://doi.org/10.3389/fpls.2022.1066752

Yano K, Morinaka Y, Wang F, Huang P, Takehara S, Hirai T, Ito A, Koketsu E, Kawamura M, Kotake K et al (2019) GWAS with principal component analysis identifies a gene comprehensively controlling rice architecture. Proc Natl Acad Sci 116:21262–21267. https://doi.org/10.1073/pnas.1904964116

Yu M, Chen G-Y (2013) Conditional QTL mapping for waterlogging tolerance in two RILs populations of wheat. SpringerPlus 2:245. https://doi.org/10.1186/2193-1801-2-245

Yu J, Pressoir G, Briggs WH, Vroh Bi I, Yamasaki M, Doebley JF, McMullen MD, Gaut BS, Nielsen DM, Holland JB et al (2006) A unified mixed-model method for association mapping that accounts for multiple levels of relatedness. Nat Genet 38:203–208. https://doi.org/10.1038/ng1702

Yu M, Mao SL, Chen GY, Liu YX, Li W, Wei YM, Liu CJ, Zheng YL (2014) QTLs for waterlogging tolerance at germination and seedling stages in a population of recombinant inbred lines derived from a cross between synthetic and cultivated wheat genotypes. J Integr Agric 13:31–39. https://doi.org/10.1016/S2095-3119(13)60354-8

Zampieri M, Ceglar A, Dentener F, Toreti A (2017) Wheat yield loss attributable to heat waves, drought and water excess at the global, national and subnational scales. Environ Res Lett 12:064008. https://doi.org/10.1088/1748-9326/aa723b

Zhang Z, Ersoz E, Lai CQ, Todhunter RJ, Tiwari HK, Gore MA, Bradbury PJ, Yu J, Arnett DK, Ordovas JM et al (2010) Mixed linear model approach adapted for genome-wide association studies. Nat Genet 42:355–360. https://doi.org/10.1038/ng.546

Zhang H, Dean L, Wang ML, Dang P, Lamb M, Chen C (2023) GWAS with principal component analysis identify QTLs associated with main peanut flavor-related traits. Front Plant Sci 14:1204415. https://doi.org/10.3389/fpls.2023.1204415

Zhang Y, Chen X, Geng S, Zhang X (2025) A review of soil waterlogging impacts, mechanisms, and adaptive strategies. Front Plant Sci 16:1545912. https://doi.org/10.3389/fpls.2025.1545912

Zhou M (2011) Accurate phenotyping reveals better QTL for waterlogging tolerance in barley. Plant Breeding 130:203–208. https://doi.org/10.1111/j.1439-0523.2010.01792.x

Zhu C, Gore M, Buckler ES, Yu J (2008) Status and prospects of association mapping in plants. Plant Genome 1:5–20. https://doi.org/10.3835/plantgenome2008.02.0089

Zohary D, Hopf M (2000) Domestication of plants in the Old World: the origin and spread of cultivated plants in West Asia, Europe, and the Nile Valley, 3rd edn. Oxford University Press, Oxford

Publisher's note Springer Nature remains neutral with regard to jurisdictional claims in published maps and institutional affiliations.

Authors and Affiliations

Anjali Khadka[1] · Anja Karine Ruud[1] · Tove Kristina Sundgren[1] · Tatiana Belova[1,2] · Morten Lillemo[1]

✉ Anja Karine Ruud
anja.ruud@nmbu.no

[1] Faculty of Biosciences, Department of Plant Sciences, Norwegian University of Life Sciences, Post Box 5003, Aas NO-1432, Norway

[2] Centre for Molecular Medicine Norway, University of Oslo, Post Box 1137, NO-0349 Oslo, Norway